Crystallography Reports, Vol. 43, No. 2, 1998, pp. 303–306. Translated from Kristallografiya, Vol. 43, No. 2, 1998, pp. 337–340.

Analysis of Intrinsic Defects in the Lithium Niobate Structure by the NMR ^{7}Li Method

E. M. Ivanova*, N. A. Sergeev, and A. V. Yatsenko***

* *Simferopol State University, Yaltinskaya ul. 4, Simferopol, 333036 Ukraine*

** *Stetin University, Stetin, Poland*

Received January 24, 1996; in final form, August 28, 1996

Abstract—The analysis of a defect structure based on two well known formulas of the congruent composition of a $LiNbO_3$ crystal has been performed. Five main variants of the defect structure are considered and used for calculating the electric-field gradient at the ^{7}Li nuclei. Based on the set of the electric-field gradient tensors, the nuclear-magnetic-resonance (NMR) spectra are simulated for the models and then compared with the experimentally observed ones. It is found that the best agreement of these data is observed for complex defects [of the type when Nb^{5+} occupies a Li^+ vacancy plus three Li^+ vacancies (in the nearest environment) plus one independent Li^+ vacancy] with due regard for mobility of the ^{7}Li nuclei within the octahedron LiO_6 under the conditions of $3Li_2O$ deficiency.

The major task in the studies of both intrinsic and impurity defects in various single crystals is associated with the choice of the complex of appropriate methods for their investigation and a correct interpretation of the data obtained. This problem acquires a specific importance in the case of a random spatial distribution of a small number of defects, when both neutron and X-ray diffraction analyses are not informative enough. The study of intrinsic defects in a $LiNbO_3$ ferroelectric is an obvious illustration of the complexity of this task, where the main data to be interpreted are the crystal density [1], the estimated energy of defect formation [2], etc.

From the standpoint of radiospectroscopy, $LiNbO_3$ single crystals are of interest, because they include three types of nuclei possessing an electrical quadrupole moment—^{93}Nb, ^{7}Li, and ^{6}Li. Any type of intrinsic defects in the $LiNbO_3$ structure specifically distort the intracrystalline electric field within a radius of $\approx$1 nm around the points of their location, and, therefore, the NMR method is extremely promising for revealing existing defects of this type. Nevertheless, an attempt to separate defects in the cation sublattice with the use of the NMR method [3] failed. A simplified analysis of the effect of intrinsic defects in the $LiNbO_3$ structure on the ^{7}Li and ^{93}Nb NMR spectra [4] gave no unambiguous results either and, in fact, only helped to choose the appropriate method for their further study. Below, we consider the results of the studies of the defect structure by the method of computer simulation of the complete NMR ^{7}Li spectrum with the use of the exact calculation of the electric-field gradient at the ^{7}Li nuclei in the ionic approximation. The calculations were made under the assumption that the effects produced by individual of defects do not overlap and thus produce no additional distortion of a structure in their nearest environment.

The convergence of the lattice sums in the calculations of electric-field gradient was checked for the undistorted $LiNbO_3$ structure. It was found that, at $R \geq 4.0$ nm (where R is the summation radius), the calculation error does not exceed 3%, and the values of the effective charges of the O^{2-} and Nb^{5+} ions are equal to $-1.46|e|$ and $+3.38|e|$, respectively (where $|e|$ is the modulus of the electron charge). In the calculations of the effective charges, it was assumed that the effective charge of Li^+ is equal to $1.00|e|$, the quadrupole moment of the ^{7}Li nucleus is $eQ = -3 \times 10^{-26}$ cm^2 $|e|$ [5], and the constant of antiscreening is $(1 - \gamma_\infty) = 0.744$. We used the experimental value of the quadrupole coupling constant $C_z = 55$ kHz [6]. It should be noted that the use of other eQ values [6] in such calculations almost did not affect the final results obtained in our work.

The calculations based on different models of defect distribution yield a set of possible electric-field gradient tensors at the ^{7}Li nuclei—from 77 to 250 various sets. The standard expression for the quadrupole shift of the transition ($\pm 3/2 \rightleftharpoons \pm 1/2$) frequency for nuclei with the spin $I = 3/2$ in the first order of the perturbation theory has the form

$$\Delta\nu = \pm\frac{C_z}{4}(3\cos^2\theta - 1 + \eta\sin^2\theta\cos 2\varphi),$$

where $C_z = \dfrac{eQV_{zz}}{h}$, $\eta = \left|\dfrac{V_{xx} - V_{yy}}{V_{zz}}\right|$, C_z is a constant of quadrupole coupling, η is the asymmetry parameter of

1063-7745/98/4302-0303$15.00 © 1998 МАИК Наука/Interperiodica Publishing

Formation of the $LiNbO_3$ defect structure

Model	Formula of the congruent composition	Variant of structure formation
1	$Li_{0.944}NbO_{2.973}$ [9]	Independent vacancies $2V_{Li}$ and V_O [2] (*a*)
		Complexes of bound vacancies $V_{Li} + V_O + V_{Li}$ (*b*)
2	$[Li_{0.941}Nb_{0.0118}]NbO_3$ [11]	Independent vacancies $4V_{Li}$ and Nb_{Li}^{5+} [2] (*c*)
		Complexes of bound vacancies ($Nb_{Li}^{5+} + 3V_{Li}$) and independent V_{Li} (*d*)
3	$[Li_{0.941}Nb_{0.059}]Nb_{0.9528}O_3$ [10]	Complexes $4(Nb_{Li}^{5+} + V_{Nb})$ and independent Nb_{Li}^{5+} [2] (*e*)

the electric-field gradient, V_{zz} is the main component of the electric-field gradient tensor in its own coordinate system, θ is an angle between the **Z**-axis of the electric-field gradient tensor and the external magnetic field $\mathbf{B}_0$, and φ is an angle between the projection of $\mathbf{B}_0$ onto the *XY* plane in the coordinate system of the electric-field gradient tensor and the **X**-axis of the electric-field gradient tensor [7]. Evidently, knowing $(V_{zz})_i$ and η_i and calculating θ_i and φ_i for the *i*th variant of the electric-field gradient tensor, we can obtain a set of the corresponding $\Delta\nu_i$ values. Taking into account that the intensities of the quadrupole satellites and the central line for the nuclei with the spin $I = 3/2$ are related as 3 : 4 : 3 and that the magnetic dipole–dipole interactions provide the Gaussian shape of the line having a width of $\delta\nu = 8.2$ kHz [8], we can restore the complete NMR ^{7}Li spectrum for any **B** orientation with respect to the threefold symmetry axis **C** of the crystal.

The existence of intrinsic defects in lithium niobate single crystals to be analyzed follows directly from two "competing" formulas for the congruent composition [9–11]. These formulas and the well-known variants of the defect structure, as well as the variants satisfying the principle of local electric neutrality of a crystal, are indicated in the table. According to the analysis made elsewhere [2], the preferable defect types are determined by model 3 indicating the formation of a local ilmenite-like structure. At the same time, the complex X-ray and neutron diffraction studies of lithium-niobate specimens of various compositions [12] favor model 2. One should also note that the formula of a congruent composition suggested in [12] differs from that indicated in the table, but it does not affect the results of the further analysis.

The complete NMR ^{7}Li spectra restored from the calculations of the electric-field gradient in variants (*a*) and (*e*) are shown in Fig. 1. It should be noted that these variants are characterized by the existence of the positions of ^{7}Li nuclei with a high C_z value (up to 300 kHz), which results in the appearance of additional satellite lines with a considerable splitting over the whole range of crystal orientations in a magnetic field and in a drastic increase of the second moment S_2 in the NMR spec-

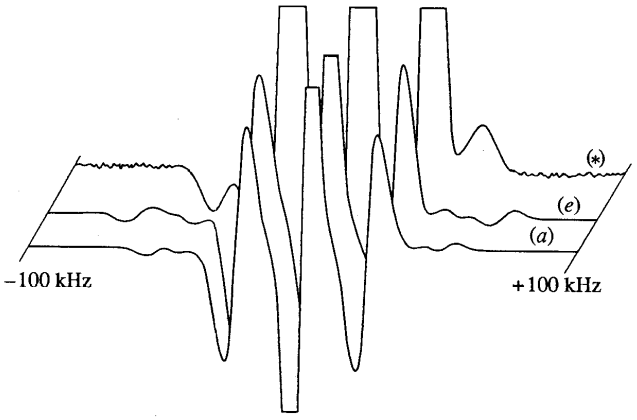

Fig. 1. NMR ^{7}Li spectra for $\alpha = 0°$ restored by using the variants (*a*) and (*e*) of the defect structure formation (see table) and the 10-times multiplied experimental spectrum (*). α is an angle between the **C**-axis of a crystal and $\mathbf{B}_0$.

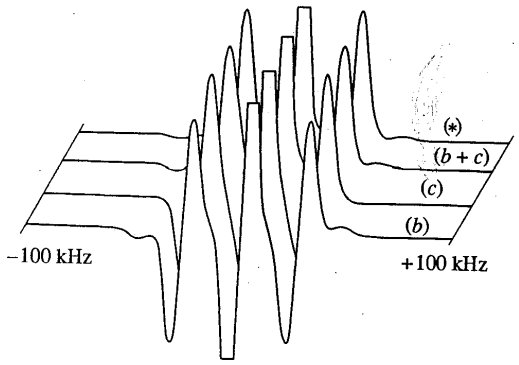

Fig. 2. NMR ^{7}Li spectra for $\alpha = 0°$ restored using the (*b*) and (*c*) variants, and the combination ($b + c$) and the experimental spectrum (*) normalized to the intensity of the central line of the spectrum.

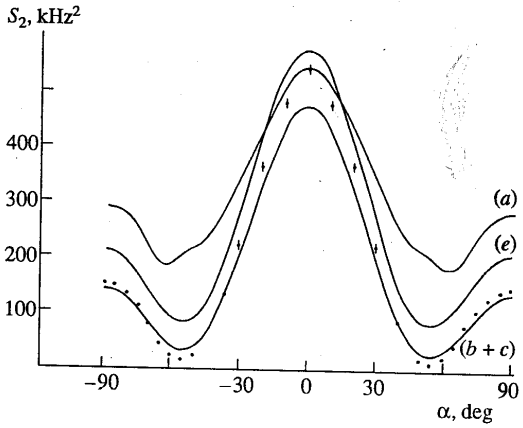

Fig. 3. Orientational dependences of the second moment S_2 of the complete NMR ^{7}Li spectrum according to the variants (*a*), (*e*), and the combination ($b + c$). Dots indicate the experimental S_2 values.

trum in a range of $\alpha \approx 55°$ in comparison with the corresponding experimental values.

The experiments were made on an NMR spectrometer with an autodyne gauge at $B_0 = 1.13$ T. In order to increase the signal-to-noise ratio, a multiple signal storage and an optimal digital filtration of spectra were used. Earlier, it was shown that Fe impurities do not affect the shape of NMR ^{7}Li spectrum over a wide concentration range [4, 13], and, therefore, a congruent $LiNbO_3$: Fe single crystal (0.07 wt % in the charge) was studied in order to reduce the time of the experiment. The additional experimental studies of the NMR ^{7}Li spectrum in the concentration range $-90° \le \alpha \le 90°$ at a scanning width of up to 400 kHz showed no additional lines [13], despite an increase of the signal-to-noise ratio up to 500 for the main quadrupole satellites (Fig. 1). The fact that no side lines of the spectrum were observed in [3] is explained by the experimental method used there—rotation at the magic angle and the use of polycrystalline specimens.

The spectra restored using the (*b*) and (*c*) variants are shown in Fig. 2. The NMR ^{7}Li spectrum, restored according to the variant (*d*), is almost identical to (*c*). The comparison of the spectrum (*b*) with the experimental one shows their qualitative consistency; however, a relative integrated intensity of the side lines (with respect to the main quadrupole satellites) is nearly two times higher than the experimentally observed intensity. In fact, one can assume that the defects in the $LiNbO_3$ structure can be described within both variants, (*b*) and (*c*), at the concentration ratio 1.1 : 1.0. This provides a rather good qualitative and quantitative agreement with the experiment (Fig. 2). The orientational dependences S_2 of the whole NMR ^{7}Li spectrum also favor such an approximation (Fig. 3).

The inconsistency between the width and the relative amplitude of side lines calculated by such a combined model and also between the S_2 variations in the range $\alpha \approx \mp 55°$ and the experimental data can be explained by the neglect of the local distortions of the crystal structure by defects and overlap of the effects caused by defects that take place in real crystals.

Nevertheless, it was found out that, when the specimen temperature is lowered from 77 to 4.2 K, the relative integrated intensities of the side lines increase by more than twice—from $6.0 \mp 1.0\%$ to $13.5 \mp 1.5\%$ [14]. It is evident that the state of the specimen and the concentration of defects of the types under study are independent of temperature. Thus, only the (*c*) and (*d*) variants of the defect structure with allowance for mobility of the Li^+ ions in LiO_6 octahedra [13] can correspond to the experimental NMR ^{7}Li data. It is the mobility of these ions that results in the quasi-powder form of the spectrum observed. The detailed analysis of the dynamic disorder of the electric-field gradient can be performed by calculating the structure of the intracrystalline field potential and then calculating the electric-field gradient for energetically favorable Li^+ ion positions. Such calculations are under way.

One should also note that the computer simulation performed for the line due to the main transition of the NMR ^{93}Nb spectrum for a similar set of structures with defects favors the variant (*d*).

ACKNOWLEDGMENTS

We are thankful to L.V. Dmitrieva (Institute of Chemistry of Silicates of the Russian Academy of Sciences) for her help in the experiments at 4.2 K.

REFERENCES

1. Nassau, K. and Lines, M.E., *J. Appl. Phys.*, 1970, vol. 41, p. 533.
2. Donnerberg, H., Tomlison, S., Catlow, C.R., and Shirmer, O.F., *Phys. Rev. B: Condens. Matter*, 1989, vol. 40, p. 1909.
3. Blümel, J., Born, E., and Metzger, T., *J. Phys. Chem. Solids*, 1994, vol. 55, p. 589.
4. Yatsenko, A.V. and Ivanova, E.M., *Fiz. Tverd. Tela* (Leningrad), 1995, vol. 37, p. 2262.
5. *Bruker Almanac, Tables*, West Germany, 1984.
6. Peterson, G.E., Bridenbaugh, P.M., and Green, P., *J. Chem. Phys.*, 1967, vol. 46, p. 4007.
7. Lundin, A.G. and Fedin, E.I., *YaMR spectroskopiya*, (NMR Spectroscopy), Moscow: Nauka, 1986.
8. Golenishchev-Kutuzov, V.A., Kopvillem, U.H., Rashkovich, L.N., and Evlanova, N.F., *Fiz. Tverd. Tela* (Leningrad), 1968, vol. 10, p. 759.
9. Bollman, W., *Cryst. Res. Technol.*, 1983, vol. 18, p. 1147.
10. Abrahams, S.C. and Marsh, P., *Acta Crystallogr., Sect. B: Struct. Sci.*, 1986, vol. 42, p. 61.
11. Lerner, P., Legras, C., and Dumas, J.P., *J. Cryst. Growth*, 1968, vol. 3/4, p. 231.
12. Iyi, N., Kitamura, K., Izumi, F., *et al.*, *J. Solid State Chem.*, 1992, vol. 101, p. 340.
13. Yatsenko, A.V. and Sergeev, N.A., *Ukr. Fiz. Zh.*, 1985, vol. 30, p. 118.
14. Dmitrieva, L.V. and Yatsenko, A.V., Abstracts of Papers, *XXXIX Soveshchanie po fizike nizkikh temperatur*, (XXXIX Meet. on Low-Temperature Physics), Kazan, 1992, part 3, p. T76.

Translated by T. Galkina